Journal of Solar Energy Research (JSER)

Journal homepage: jser.ut.ac.ir

AN Experimental Study of the Performance of a Solar Flat Plate Collector with Triangular Geometry

Mojtaba Moravej[a]

[a]*Mechanical Engineering Department of Payame noor University, Iran.*

Received: 2020-10-06
Accepted: 2021-07-11

Abstract

The flat plate collector is the most famous and simplest type of solar collectors that is used as a water heater. In this study, a solar flat plate collector with triangular geometry and with zigzag and non-riser tubes was experimentally examined. To assess the collector, the ASHRAE standard was used in hot and dry climate conditions. The test site was located in southwestern Iran and was tested in the early months from March to June 2020. The measured parameters include the environmental and thermal parameters of the collector and the fluid, and the best data have been selected and presented. The results of the study showed that the collector had a suitable efficiency; the lowest recorded value was 32% and the highest was 58.9 %. Hence, It could be used as a solar water heating system in both domestic and industrial sectors. In the pressure drop testing, the results showed that in all flow rates used, the pressure drop in the collector was less than 0.1 bar. Also, the performance of the collector was presented based on environmental variables such as temperature and radiation, as well as fluid variables such as input temperature and flow rate.

Keywords: Flat plate, Triangular solar collector, Efficiency, Experimental.

1. Introduction

The need to expand and develop renewable energy is not hidden from anyone in the world today. It is safe to say that the most practical and well-known type of renewable energy is solar energy, which has long been used by humans thousands of years ago. Solar energy can be used in two common forms of energy: heat and photovoltaic. In solar thermal energy a heat exchanger called collector is used. In fact, a solar collector is a thermal device for absorbing solar radiation and converting it into the required heat in a system such as a water heater [1-3]. Collector efficiency enhancement is one of the main subjects in solar thermal engineering. Cosequently, there are many ways to enhance collector efficiency. Changing the geometry of the solar collector and increasing the thermal specification of the coolant such as nanofluid are two key ways to solve this problem [4-6].

Many researchers around the world have been researching about the enhancing of collector performance. Saffarian et al. [7] conducted a comprehensive study on the types of solar flat plate collectors based on the arrangement of pipes in a conventional flat plate collector, including the study

*moravej60@pnu.ac.ir

of heat transfer, pressure drop and their efficiency. Water and a variety of nanofluids were used to determine the type of fluid and its concentration as important parameters of measurement, and finally concluded that nanocidal copper oxide with a concentration of 4% could be the best option to increase the efficiency of the solar collector. Also, in their research, they determined the type of pipe arrangement and how it will increase efficiency with different arrangements and connections of pipes. In another study, Mohamed et al. [8] studied a special form of using flat plate collector in an energy storage system. Their study was conducted in Egypt, and they showed that in summer the maximum energy save gained by their collector was 16.11 MJ/day and in winter the minimum value was about 10.26 MJ/day .Mirzaei [9] conducted an experimental study of copper nanocidal oxide on a solar bed plate collector. In this study, he used a collector with an area of 1.51 square meters and used nanoscale with a volumetric concentration of 1% in different flow rate between 1 to 4 liters per minute in his experiments and proved that the performance of the solar collector in low flow rate is nonlinear. And its behavior in higher quasi-linear Flow rate also showed that the increase in the yield of the collector using nanofluid can be increased up to 55%. This value is possible in 4-liter-per-minute flow rate. Sint et al. [10] performed a theoretical analysis to determine the efficiency of a CuO-water nanofluid based-flat plate solar collector for domestic solar water heating system in Myanmar. They proved that the use of CuO-water nanofluid as coolant could increase the performance of flat-plate collector up to 5%. Visa et al. [11] introduced a triangular solar collector in the range of flat plate type. They designed it by ANSYS software and made it in small size with the area less than 0.1 m^2 to use in building facades. The collector was made in three different colors - black, green and orange- that have 55%, 42% and 35% performance respectively.

Goudarzi et al. [12] had a laboratory study on a solar cylindrical collector with spiral tubes. The nanofluid used in this study was copper oxide based on water fluid. The test was besed on the standard of ASHRAE. The flow rates ranged from 0.0083-0.033 kg/s and the nanofluid concentration was 0.1, 0.2 and 0.4% by weight. Maximum efficiency increased in flow rate 0.0083 and the concentration 0.1, which was almost 25.6% higher.

In an interesting study, Verma et al. [13] investigated the use of different nanofluids in the solar flat plate collector. In fact they used hybrid nanofluids with water as base fluid and nanoparticles included CuO, and MgO with multy carbon nanotubes. The concentrations used were between 0.25% to 2% , and the fluid flow rates were between 0.5 to 2 lpm. They showed that using hybrid MgO-MWCNTs nanofluids yields approximately 25% and in combination hybrid CuO-MWCNTs nanofluids more than 16% is added to the yield of the collector.

Noghrehabadi et al. [14, 15] also examined an experimental 3D card with conical geometry and spiral tubes experimentally in the laboratory. In this study, a cone-shaped shell was used as the adsorbent and tubes containing the fluid in a spiral from the bottom to the top point of collector. The results illustrated that the maximum outlet temperature was more than 77^0C and the maximum efficiency was about 60%. Moravej et al. [16] examined a linear and non-riser flat plate collector spiral tube collector experimentally according to the ASHRAE standard. The results showed that the performance of a circular collector can be greater than that of other flat plate collectors. The main reason being the presence of secondary currents in the spiral tubes. Kiliç et al. [17] had experimental investigation of using TiO_2/water nanofluid in a flat plate collector according to ISO 9806 standard. In this study the incident radiation of sun was more than 850 and reached to 1170 but the collector efficiency was less than 50%. Farajzadeh et al. [18] experimentally and theoretically studied hybrid nanfluid in a flat plate collector. They concluded that using 0.1% (wt) of Al_2O_3-TiO_2-water nanfluid can increase the thermal efficiency of a flat plate collector by about 26%.

One of the geometries that can be widely used in solar water heating systems, especially integrated and combined, is the triangular geometry for the flat plate collector. So far, limited experimental research has been done on this geometry. So in this study, a collector of solar bed screen with triangular geometry, without riser and with U-shaped pipes was

designed and made by the author. It was tested in the weather conditions of cream and dryness according to the standard of the test and the effect of different parameters on its performance.

2. Materials and Methods

For experimental evaluation, a collector with a triangular geometry has been designed and made by the author at Payame Noor University of Aghajari the specifications of which are presented in Table 1. This collector has copper coil tubes from the inlet to the collector outlet and does not have any riser. For complete insulation, the absorbent plate and tubes are mounted on a wooden frame and then placed inside an aluminum frame and covered with flat glass. For sealing, all wood, metal and glass seams were sealed with silicone glue. Fig. 1 shows the triangular solar collector with absorber, tank and frames.

2.1. Test procedure

The laboratory layout and the method of testing and data collection, along with how the collector is located in the process of absorbing radiation from the sun and transferring heat to the operating fluid, are presented in Fig. 2. According to this figure, the working fluid leaves the tank and enter the pump inlet. After pumping, the amount of flow is measured and the working fluid is entered at the inlet of the triangular collector and passed through the collector pipes. The values of fluid pressure and temperature at the collector inlet and outlet are measured. It is common that environmental parameters such as humidity, ambient temperature, wind speed and sun radiation outside the collector and piping are measured independently. All of devices such as the pump, the flow meter and the pressure gauges are illustrated and numbered in Fig. 2.

Figure 1. Photo of the triangular flat plate collector

Table 1. Specification of triangular collector

Specifications	Materials	Dimensions and units
Type	Triangular flat plat collector	Black color
Frame	Aluminum-white color	Frame area=0.606 m^2
Absorber	Ordinary iron sheet with 1.25 mm thickness	Absorber area=0.500 m^2 The triangle with 80cm base and 125cm height.
Glazing	Single flat glass	6 mm thickness
Collector tilt angle	45 degree with ground	-
Insolation	Wood	thickness=22 mm
Weight	Total weight without fluid	28 kg
Piping	Cupper tubes	Inner diameter=8.6 mm
Retaining structure	Usual iron	25kg

Table 2. ASHRAE Standard conditions [19]

Parameters	ASHRAE Standard	Unit
Inlet temperature variation	±1	°C
Outlet temperature variation	±0.5	°C
Ambient temperature	At a height of 120 cm from the ground and at a	°C
Ambient temperature variation	±0.5	°C
Flow rate variation	±1	%
Incident sun radiation	±50	W/m^2

Table 3. Environmental conditions according to standard [19]

Variable	Absolute limits
Total solar irradiance normal to sun(W/m^2)	790(minimum)
Diffuse fraction (%)	20
Wind speed	2.3<U<4.8
Incidence angle modifier	98%<normal incidence, value<102%

According to Fig. 2, it is clear that the working fluid heats up in the initial (cold) state after entering the collector by passing through the pipes connected to the adsorbent and the hot fluid exits the collector. The ASHRAE standard is used, the conditions of which can be seen in Tables 2&3. In order to measure the test data, various measuring instruments were used, the specifications of each are presented in Table 4. In short, it can be said that the amount of heating of the outlet fluid relative to the inlet fluid is equal to the amount of energy obtained from the collector, which is obtained by measuring the thermodynamic and fluid properties of the operating fluid before and after the collector.

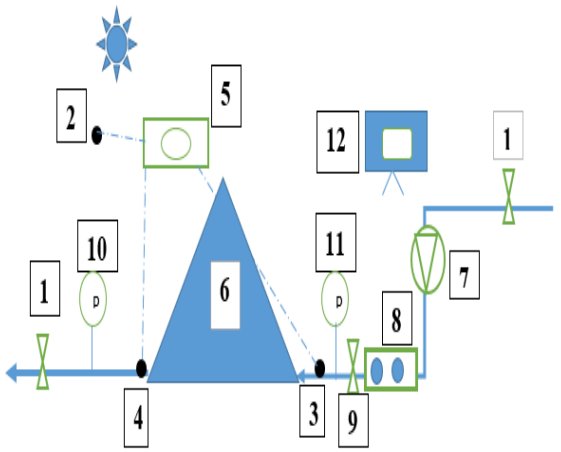

Number	Name of device	Number	Name of device	Number	Name of device
1	Valve	6	Triangular collector	9	Control valve
2,3,4	Thermocouples	7	Pump	10, 11	Pressure gauge
5	Data logger	8	Flow meter	12	Logger of wind and humidity

Figure 2. Setup of the experiment

Figure 3. Actual photo of measurement devices

All measuring devices were calibrated before the start of the experiments and collected and cleaned at the end of the day after the experiment and reused the next day. Fig. 3 illustrate the measuring devices that

are used in this study, and Table 4 shows the specifications of these measurement devices. For better evaluation, triangular collector is located on the roof of the university's educational building and the data are recorded simultaneously. The experimental site at Payame Noor University in Aghajari, a city in southern Iran, at an altitude of 131 meters above sea level, with a longitude of 30 degrees and 69 minutes north and a latitude of 49 degrees and 82 minutes east. This city have hot and dry climate and in summer ambient temperatures will be over 40 ^{0}C. The collector was active in the early hours of the morning until evening, and data was collected during the 2020s. In order to evaluate more accurately and remove inaccurate data, the time provided in the results is from 10 am to 4 pm. The performance of the collector is measured according to the ASHRAE standard. The collectors are continuously exposed to sunlight and the fluid flow is generated by the electric diaphragm pump. The data is recorded in stable and quasi-stable conditions. Experiments have also been repeated regularly and in different conditions of data collection.

Table 4**.** Specifications of the measurement devices

Devices	Model	Parameter	Unit	Accuracy
Thermometer	lutron	Fluid and ambient teperatures	^{0} C	0.1
Rotameter	Km450	Flow rate	gpm	0.1
Wind speed meter	lutron	Wind speed	m/s	0.1
Solar power meter	Tes-132	Incident sun radiation	W/ m^2	1
Pressure gauge	Pekunzi	Pressure of fluid	bar	0.1
Humidity meter	Htc-110	Humidity	%	1%
Thermocouple	K type	temperature	mV/ ^{0} C	0.004

2.2. Collector time constant

One of the special features of any solar collector is that it somehow introduces the heat capacity of the collectors and the operation of the collector in transient conditions and is usually measured in two ways. One measurement method is that if a collector is in operation and immediately a black barrier or fabric is exposed to the collector, how long does it take for the outlet fluid temperature to reach 63% of the outlet temperature before covered. Eq. (1) is used to calculate time constants [3, 19].

$$\frac{e}{T_{O,i} - T_i} = \frac{1}{T_{O,\Gamma} - T_i} \quad (1)$$

Where Ti is the inlet temperature to the collector, $T_{O,i}$ is the output temperature of the collector in steady state and $T_{O,\Gamma}$ is the output temperature of the collector after time Γ [3, 19].

2.3. Govering Equations

According to the ASHRAE standard, the efficiency of the collector is based on the amount of radiation and energy received by the collector, the temperature difference between the inlet and outlet of the collector, the thermal characteristics of the operating fluid and the flow rate of the fluid. In fact, the efficiency can be calculated by considering the heat ratio obtained from the collector by the operating fluid and the heat and solar energy reached. The useful energy obtained by the fluid passing through the collector is:

$$Q_u = \dot{m} C_p (T_o - T_i) \quad (2)$$

Where Q_U is the amount of energy obtained from the collector, $\dot{m}$ is the flow rate of the operating fluid, Cp is the specific heat of the operating fluid, and T_{in},

T_o are the input and output temperatures of the operating fluid, respectively.

The useful energy obtained by the collector in terms of the amount of solar radiation entering and thermal losses from the collector body is [20]:

$$Q_u = A_p F_R [Rad - U_l(T_{in} - T_a)] \quad (3)$$

Where Ap is the FR adsorption surface of the heat dissipation coefficient, Rad is the amount of solar radiation, UL is the total temperature drop coefficient and Ta is the ambient temperature. The heat dissipation coefficient can also be defined based on Equation (4) [16, 20].

$$F_R = \frac{\dot{m}C_p}{U_l A_p}\left[1 - \exp\left(\frac{-F' U_l A_p}{\dot{m}C_p}\right)\right] \quad (4)$$

Where the collector coefficient is. In stable mode, the useful energy received by the collector is:

$$Q_u = A_p Rad - U_l A_p (T_p - T_a) \quad (5)$$

Where Tp is the temperature of the adsorbent plate and U_l is the total drop of the collector [20]. Now, with the help of the data obtained from the measurement every 15 minutes, which includes the inlet and outlet water temperature, the ambient temperature and the intensity of the received radiation, and the placement in to Equaion (6) the collector efficiency is calculated. Factors influencing the rate of return include mass discharge, the difference between the temperature of the outlet and inlet water, and the intensity of the total radiation received, which are analyzed here [20].

$$\eta_i = \frac{Q_u}{A_c Rad} = \frac{\dot{m}C_p(T_o - T_i)}{Rad} \quad (6)$$

$$\eta_i = F_R(\tau\alpha) - F_R U_L\left(\frac{T_i - T_a}{Rad}\right) \quad (7)$$

According to Equation (5), if the yield values are plotted as a function and based on the variable (Ti-Ta) / Rad), the resulting curve consists of a line whose intersection with the vertical axis is the value of $F_R(\tau\alpha)$. This value represents the maximum collector efficiency and occurs when the temperature of the incoming fluid to the collector is equal to the ambient temperature. The intersection of this line with the horizontal axis is called the collector stagnation point at which the cumulative efficiency reaches zero and occurs when the flow rate in Flow rate becomes zero. The slope of the line is equal to $F_R U_L$, which represents the amount of energy loss from solar collection.

2.4. Uncertainty analysis

It is clear that errors in all measurements are inevitable in experiments. The types of errors in calculations and measurements in the present study include device calibration error, visual reading of cultivars, as well as the type of devices used. Data errors include temperature, solar radiation, area and flow rate measurement [21]. To calculate the uncertainty in the experiments, the ROOT SUM

SQAURE METHOD (RSSM) method was used, which is presented in Equation (8).

$$S = \sqrt{(\frac{\Delta u_1}{u_1})^2 + (\frac{\Delta u_2}{u_2})^2 + (\frac{\Delta u_3}{u})^2 + \cdots} \quad (8)$$

Therefore, for the present study, according to Equation (6), we can write:

$$S_\eta = \sqrt{(\frac{\Delta \dot{m}}{\dot{m}})^2 + (\frac{\Delta DA}{DA})^2 + (\frac{\Delta DT}{DT})^2 + (\frac{\Delta R}{R_a} \quad (9)$$

According to the calculations and measurements, Table 5, the amount of uncertainty calculated for the above data for Flow rate, area, temperature and solar radiation, respectively, is 5.5%, 0.01%, 0.2% and 3.1%, respectively. These numbers in relation to (9) can be claimed that the uncertainty of calculating the efficiency of collectors is about 6.3%.

Table 5. Uncertainty results for the measurements.

Parameter	**Uncertainty (%)**
Volumetric flow rate	±5.5
Solar radiation	±3.1
Absorber area	±0.01
Difference between inlet and outlet temperatures	±0.2

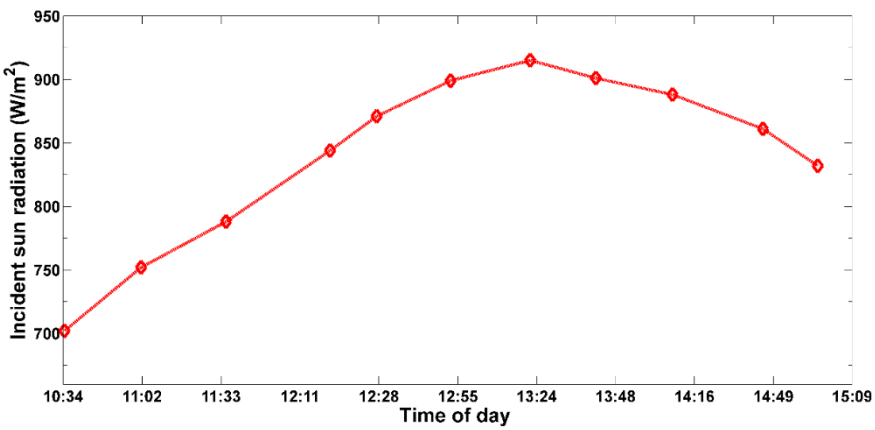

Figure 4. Incident sun radiation via the tests (April 2020)

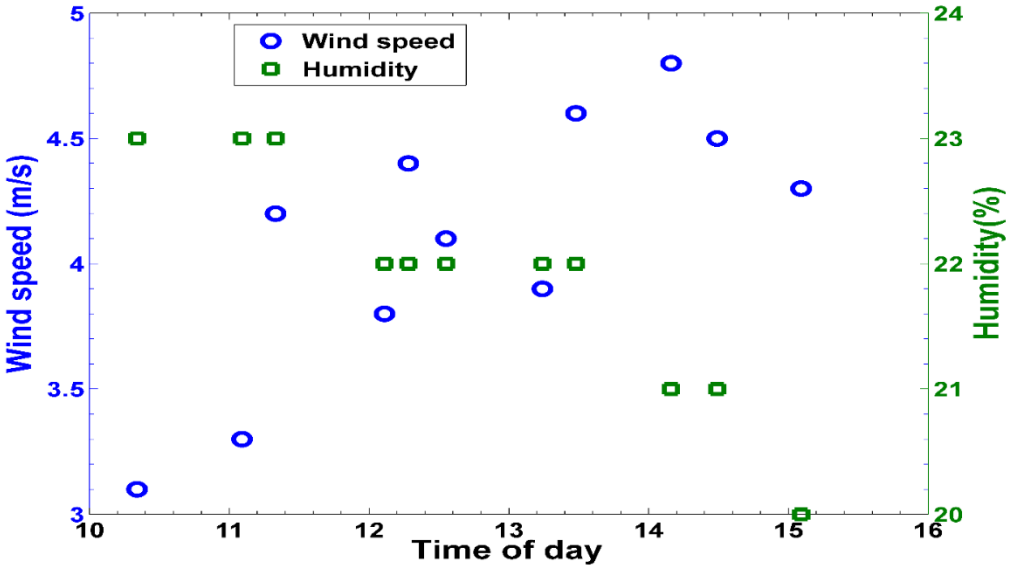

Figure 5. Wind speed and ambient humidity during the test day (April 2020)

3.Results and Discussions

Fig. 4 shows the amount of incident solar radiation reaching the vertical surface of the triangular collector whose data are obtained in clear, cloudless, and completely sunny weather (in April 2020).This radiation is the sum of the beam, deffuse, and reflective radiation energy of other objects close to the collector, which is measured directly by the radiation meter. As can be seen in this figure, the radiation is displayed before noon and in the afternoon of the sun, which has an upward trend before noon and then decreases. In the horizontal axis of this chart, the time is presented in terms of hour and minute and in specific intervals, which includes accurate data collection during the test day. According to the standard of the ASHRAE, the radiation before these times and less than 700 watts per square meter is not accurate to evaluate the efficiency of the collector.

Fig. 5 show wind speed and relative humidity, respectively, at the time and place of the experiment. Although the tests have been performed on several days, the best data for this chart and other cases have been selected and presented. To measure the wind speed, the wind gauge was used at different angles and at a distance of at least two meters from the collector, and the highest speed recorded at that time provided the experiment. In total, the highest wind speed recorded at the test site was 9.8 m/s on different days from March to June. In Fig. 6, the relative humidity of the air around the test site is measured and displayed. According to this chart and the hot dryness of the test site, the humidity was generally low during the test days.

Fig. 6 shows the ambient temperature chart, input and output temperature of the triangular collector. Due to the time and geographic area tested, the ambient air temperature was very high during these months, and sometimes reached above 50 degrees Celsius, which actually caused the data to be windy. In Fig. 7, in addition to the ambient temperature, the inlet and outlet temperatures of the collector are also provided. Actually, the closer the inlet temperature to the collector is to ambient temperature, the better the efficiency of the collector. This condition is best achieved especiall before the noon.

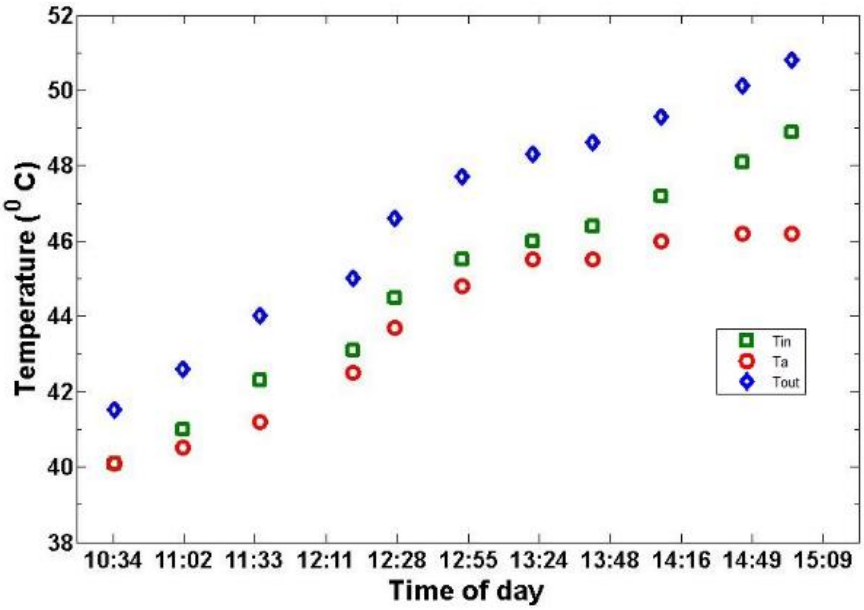

Figure 6. Temperature variation during the test day

Fig. 7 shows the efficiency and thermal performance of the collector based on the data obtained from the previous diagrams and Equation (6). What is clear is that as the radiation increases during the day and getting close to the maximum level occuring at noon in the sun, the amount of collector efficiency increases and then declines, which is similar to previous research [1-5]. In addition to reduction of radiation and heat transfer, the reason for the decrease in efficiency is the increase in ambient temperature. In the afternoon, with increasing ambient temperature and increasing the difference between the inlet temperature to the collector and the ambient temperature, the efficiency of the collector decreases. Reducing the temperature difference between the ambient temperature and the temperature entering the collector in the afternoon is more difficult because the temperature of the exit from the tank is generally high and reducing it to the ambient temperature is both time consuming and expensive. Fig. 8 shows the efficiency and performance of the triangular collector in terms of flow rate. What is clear in this figure is that as the flow rate increases, the collector efficiency increases. The reason for this behavior is that as the flow rate increases, the fluid velocity and consequently the Reynolds number increases, causing the heat transfer from the pipe wall to the operating fluid to grow, which is similar to previous research and results presented in references [3, 9, 12].

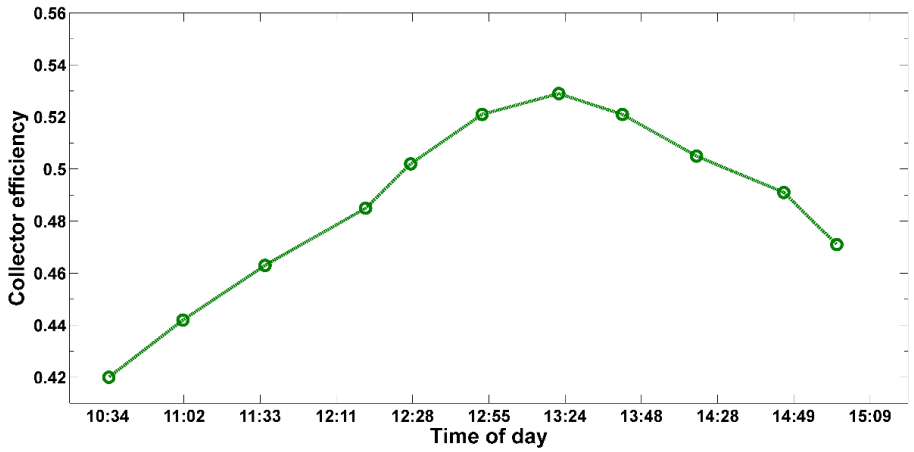

Figure 7. Collector efficiency during the time of the day

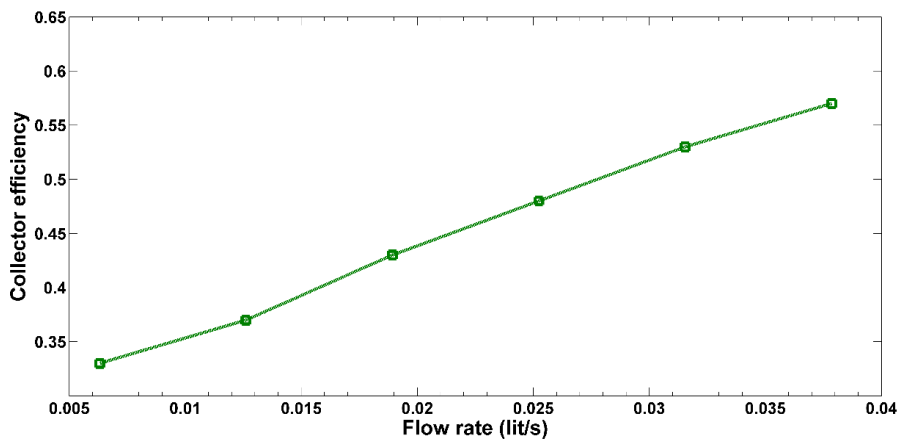

Figure 8. The effect of flow rate on the collector efficiency

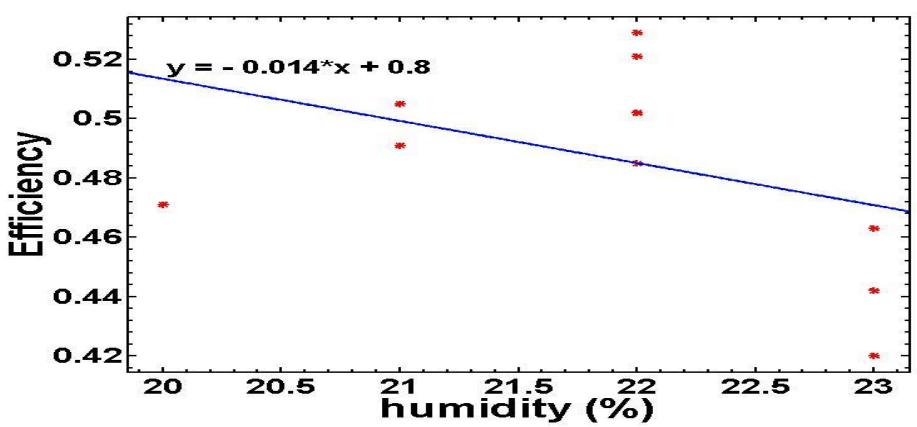

Figure 9. Effect of ambient humidity on collector efficiency

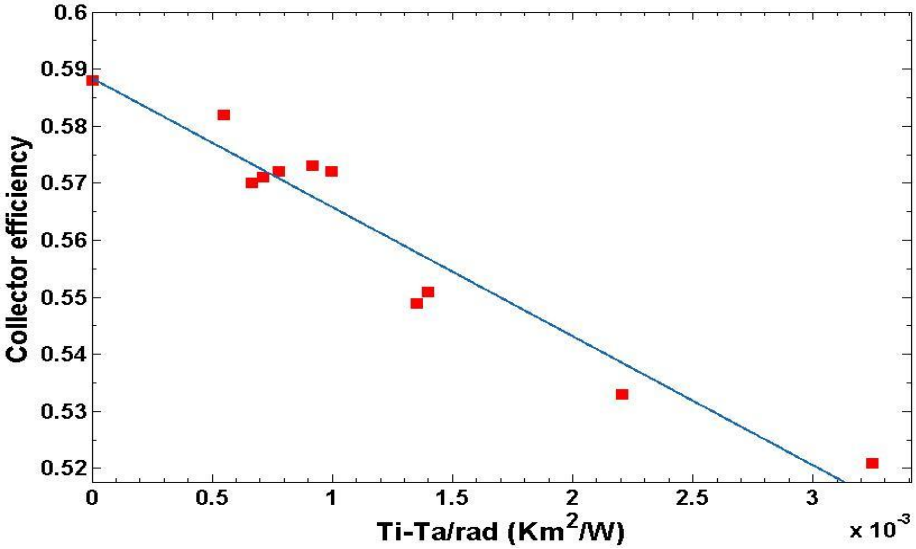

Figure 10. The regression of collector efficiency via $\frac{Ti-Ta}{rad}$ parameter

Table 6. Linear curve fitting of figure 10

Flow rate (kg/s)	$F_R(\tau\alpha)$	F_RU_L	R^2	SSE	RMSE
0.037854	0.5884	22.62	0.932	0.0002955	0.00573

Fig. 9 illustrate the effect of ambient humidity on thermal performance of triangular collector. In this chart, due to variation range, the linear curve fitting is used and the linear fitted equation is cleared in the chart. According to this figure, when the ambient humidity increase, the collector efficiency was decrease in a small slope. This trend can be explained by the effect of humidity in heat loss of collector and decreasing in gained solar beam.

According to Equation (7), it can be said that there is a linear relationship between collector efficiency and the $\frac{Ti-Ta}{rad}$ parameter, so considering this parameter and efficiency based on the obtained data, a linear regression can be approximated and the values F_RU_L and $F_R(\tau\alpha)$ in calculate the relationship of 7. This regression is mentioned in Fig. 10 and their values are shown in Table 6. Regression is done by MATLAB software and the coefficients of regression calculation such as the correlation coefficient are shown in Table 6. In fact, $F_R(\tau\alpha)$ is the maximum value of the collector efficiency in a particular discharge, which is the same as the value obtained from the intersection of the vertical line diagram with the vertical axis, and is obtained when the difference in ambient temperature with the inlet temperature to the collector is zero.

The slope of the line is equal to F_RU_L or the same energy loss coefficient in the collector, the higher the heat loss in the collector [16, 22, 23, 24].Another variable studied in this study and measured in experiments was fluid pressure, i.e. pressure drop in the collector. Due to the spiral and zigzag pipes in the collector, it seems that the pressure drop in the collector is a significant amount and its measurement seems necessary. Therefore, using two barometers placed on both sides of the collector at the inlet and outlet of the fluid, the pressure drop was checked in the collector. The results of the pressure drop test

showed that in all flow rates, it was found that the value was not significant and was less than 0.1 bar.

4.Conclusions

In this paper, a collector type of flat plate without trace and riser with triangular geometry and U-shaped pipes designed and made by the author, has been experimentally tested in hot and dry weather conditions in southern Iran. The results of the study show that with the increase in flow rate, the increase in efficiency is noticeable and behaves ascending. Also, with increasing time from morning to noon, the amount of radiation and thus the efficiency of the collector increases, but it decreases in the afternoon, which is due to the decrease in radiation and high temperature difference between the ambient temperature and the temperature entering the collector. An important advantage of this collector is the low pressure difference and consequently the reduction of pumping costs and related applications, so that even in most flow rates, the pressure difference has been much less than 0.1 bar.

Nomenclature		
Ap	Absorber area	(m^2)
C_p	Specific heat for fluid	(J/Kg k)
$C_{p,nf}$	Specific heat for nsnofluid	(J/Kg k)
$C_{p,np}$	Specific heat for nanoparticles	(J/Kg k)
$C_{p,bf}$	Specific heat for basefluid	(J/Kg k)
DT	Difference between inlet-outlet temperaure	(^{0}C)
F_R	Coefficient of energy in collector	-
F'	Collector coefficient	-
Rad	Incident sun radiation	(W/m^2)
$\dot{m}$	Mass flow rate	(Kg/s)
Q_u	Useful energy gained from collector	(W)
S_η	Uncertainty	%
T_a	Ambient temperature	(^{0}C)
T_{in}	Inlet temperature to the collector	(^{0}C)
T_{out}	outlet temperature of the collector	(^{0}C)
T_P	Absorber temperature	(^{0}C)
U_L	Total loss energy coefficient	(W/m^2 K)
$T\alpha$	Absorption-transmittance product	-
μ	Nanofluid concentration	%
η_i	Instantaneous collector efficiency	%

References

1.Rezvanpour, M., D. Borooghani, F. Torabi, and M. Pazoki, *Using CaCl2· 6H2O as a phase change material for thermo-regulation and enhancing photovoltaic panels' conversion efficiency: Experimental study and TRNSYS validation.* Renewable Energy, 2020. **146**: p. 1907-1921.

*2.*Braun, H. *The phoenix project: Shifting to a solar hydrogen economy by 2020*. Chemical Industry and Chemical Engineering Quarterly/CICEQ, 2008. **14**: p. 107-118.

3. Noghrehabadi, A., E. Hajidavalloo, and M. Moravej, *Experimental investigation of efficiency of square flat-plate solar collector using SiO2/water nanofluid*. Case Studies in Thermal Engineering, 2016. **8**: p. 378-386.

4. Menni, Y., A. Azzi, and A. J. Chamkha, *A review of solar energy collectors: models and applications.* Journal of Applied and Computational Mechanics, 2018. **4**: p. 375-401.

5. Ahmed, O. K. *A numerical and experimental investigation for a triangular storage collector*. Solar Energy, 2018. **171**: p. 884-892.

6. Manikandan, S. P., R. Baskar, *Heat transfer studies in compact heat exchanger using Zno and TiO2 nanofluids in ethylene glycol/water*. Chemical Industry and Chemical Engineering Quarterly, 2018. **24**: p. 309-318.

7. Saffarian, M. R., M. Moravej, and M. H. Doranehgard, *Heat transfer enhancement in a flat plate solar collector with different flow path shapes using nanofluid.* Renewable Energy, 2020. **146**: p. 2316-2329.

8. Mohamed, M. M., N. H. Mahmoud, and M. A. Farahat, *Energy storage system with flat plate solar collector and water-ZnO nanofluid.* Solar Energy, 2020. **202**: p. 25-31.

9. Mirzaei, M. *Experimental investigation of CuO nanofluid in the thermal characteristics of a flat plate solar collector*. Environmental Progress & Sustainable Energy, 2019. **38**: p. 260-267.

10. Sint, N. K. C., I. A. Choudhury, H. H. Masjuki, and H. Aoyama, *Theoretical analysis to determine the efficiency of a CuO-water nanofluid based-flat plate solar collector for domestic solar water heating system in Myanmar*. Solar Energy, 2017. **155**: p. 608-619.

11. Visa, I., M. Moldovan, and A. Duta, *Novel triangle flat plate solar thermal collector for facades integration.* Renewable Energy, 2019. **143**: p. 252-262.

12. Goudarzi, K., E. Shojaeizadeh, and F. Nejati, *An experimental investigation on the simultaneous effect of CuO–H2O nanofluid and receiver helical pipe on the thermal efficiency of a cylindrical solar collector*. Applied Thermal Engineering, 2014. **73**: p. 1236-1243.

13. Verma, S. K., A. K. Tiwari, S. Tiwari, and D. S. Chauhan, *Performance analysis of hybrid nanofluids in flat plate solar collector as an advanced working fluid.* Solar Energy, 2018. **167**: p. 231-241.

14. Noghrehabadi, A., E. Hajidavalloo, and M. Moravej, *An experimental investigation of performance of a 3-D solar conical collector at different flow rates.* Journal of Heat and Mass Transfer Research, 2016. **3**: p. 57-66.

15. Noghrehabadi, A., E. Hajidavalloo, and M. Moravej, *An experimental investigation on the performance of a symmetric conical solar collector using SiO2/water nanofluid.* Challenges in Nano and Micro Scale Science and Technology, 2016. **5**: p. 23-29.

16. Moravej, M., M. R. Saffarian,L. K. Li, M. H. Doranehgard, and Q. Xiong, *Experimental investigation of circular flat-panel collector performance with spiral pipes.* Journal of Thermal Analysis and Calorimetry, 2019. p. 1-8.

17. Kiliç, F., T. Menlik, and A. Sözen, *Effect of titanium dioxide/water nanofluid use on thermal performance of the flat plate solar collector*. Solar Energy, 2018. **164**: p. 101-108.

18. Farajzadeh, E., S. Movahed, and R. Hosseini, *Experimental and numerical investigations on the effect of Al2O3/TiO2H2O nanofluids on thermal efficiency of the flat plate solar collector*. Renewable Energy, 2018. 118: p.122-130.

19. ASHRAE, *Standard 93-2010– Methods of Testing to Determine the Thermal Performance of Solar Collectors (ANSI Approved),* ANSI/ASHRAE Standard 93-2010 (R2014). ASHRAE Inc., Atlanta, USA

20. Duffie, J. A., W. A. Beckman, and N. Blair, *Solar engineering of thermal processes, photovoltaics and wind.* John Wiley & Sons, 2020.

21. Moradi, R., M.R. Saffarian, and M. Behbahani-Nejad, *Experimental study of an air humidity absorption cycle based on the MHI*. Journal of Thermal Analysis and Calorimetry, 2019. p.1-9.

22. Moravej, M., F. Namdarnia, *Experimental Investigation of the Efficiency of a Semi-Spherical*

Solar piping Collector. Journal of Renewable Energy and Environment, 2018. **5:** p. 22-30.

23. Tong, Y., H. Lee, W. Kang, and H. Cho, *Energy and exergy comparison of a flat-plate solar collector using water, Al2O3 nanofluid, and CuO nanofluid*. Applied Thermal Engineering, 2019. **159:** 113959.

24. Noghrehabadi, A., E. Hajidavaloo, M. Moravej, *and A. Esmailinasab, An experimental study of the thermal performance of the square and rhombic solar collectors.* Thermal Science, 2018. **22:** p. 487-494.